Beam Aggregation for Instantaneous Link Recovery in Millimeter Wave Communications

Mohammed Jasim, Adel Aldalbahi[+], Hazim Shakhatreh[*]
Department of Electrical and Computer Engineering, Valparaiso University, Valparaiso, IN, USA
[+]Department of Electrical Engineering, King Faisal University, Al Ahsa, KSA
[*]Departmentt of Electrical and Computer Engineering, New Jersey Institute of Technology, Newark, NJ, USA
Email: mohammed.jasim@valpo.edu, aaldalbahi@kfu.edu.sa, hms35@njit.edu

***Abstract*—Cellular networks at millimeter wave frequencies experience tremendous propagation impairments and channel fluctuations. One major challenge here is the aggregated path loss levels attributed to obstacles of various shapes and density in the propagation links, i.e., link blockage. Therefore, once the base and mobile stations establish the optimum beamforming and combining vectors during the initial beam access procedure in the control-plane, efficient link maintenance techniques are required to maintain communication sessions with sufficient signal levels at various blockage densities. Hence this paper presents a novel link recovery scheme based upon beam aggregation during link transitions from line-of-sight to non-line-of-sight (NLoS) environments. The proposed scheme utilizes circular antenna arrays and hybrid beamforming designs to achieve near-instantaneous recovery times without the need for repeated beam scanning. Simulation results show that the proposed recovery scheme exhibits significant improvements compared to alternative traditional methods in terms of signal-to-noise ratios and recovery times.**

***Index Terms*—Millimeter wave, beam aggregation, link maintenance, link recovery, circular arrays, hybrid beamforming, recovery times**

I. Introduction

Millimeter wave (mmWave) bands constitute a key component of 5G cellular systems for enhanced mobile broadband (eMBB) as proposed in [1]. Now despite the tremendous merits of this technology in terms of abundant contiguous spectrum and miniature array dimensions, several challenges exists prior to its deployment as a standalone network, in particular, increased path and penetration losses. Hence phased arrays and beamforming technologies have become a major component of mmWave networks to compensate for channel fluctuations and propagation impairments, i.e., introducing aggregated gains. Consequently, directional transmission and reception modes are adopted during control- and data-planes instead of omnidirectional transmission modes in conventional microwave networks, i.e., in particular at the mobile station (MS). This in return results in initial beam access challenges, since narrow beams are utilizes for data transmission. Therefore, the base station (BS) and MS are required to conduct exhaustive spatial search, i.e., to determine the direction of the primary beam associated with the optimum beamforming and combining vectors that return the highest received signal level. This search yields excessive beam access times in mmWave networks. Now several studies have developed adaptive and efficient initial beam access schemes. Foremost, work in [2]-[5] proposes fast access methods based upon Hooke Jeeves, Coordinated Pattern Search, Luus Jaakola, and Nelder Mead meta-heuristics methods, respectively, in efforts to reduce access times and control-plane latencies.

Furthermore, mmWave links are highly sensitivity to obstacles in the propagation channel, since they result in signal degradation during transition from line-of-sight (LoS) to non-line-of-sight (NLoS), i.e., resulting in blockage. As a result, signal-to-noise ratio (SNR), Shannon capacity and spectral efficiency are significantly reduced. Consequently, received signal levels can decay below receiver sensitivity, which yields blockage-based outages [7]. Therefore, one major challenge here is the subsequent stage to initial beam access, termed as *link maintenance*.

Now traditional link recovery techniques restart the spatial beam scanning procedure when the optimum link between the BS and MS degrades, e.g., due to channel blockage. Foremost, the hierarchical codebook-based access schemes in [2]-[5] determine new optimum beam directions. Meanwhile, other approaches examine adjacent directions to the failed beams [6]. However, the aforementioned techniques require prolonged recovery times, which can result in connection drops.

Therefore, fast and efficient link recovery schemes are required to maintain mmWave communication sessions after the initial access control- and data-planes. In particular, once the received signal level associated with the optimum beamforming and combining vectors (also known as the primary beams) is degraded, link recovery schemes are necessary to compensate for this degradation, i.e., considering recovery times due to the short coherence times affiliated with mmWave systems.

Hence this paper proposes novel link recovery scheme based upon beam aggregation to enhance received signal levels and compensate for increased blockage path losses. Here circular arrays and hybrid beamforming architectures are utilized for the first time to radiate overlaid beams at the same directions to enhance the signal affiliated with the primary beam during initial beam access. Namely, dual aggregated beams are generated from the hybrid beamformer in the same direction of the primary beam, i.e., to enhance the received signal level, as shown in Figure 1. The proposed scheme features near–

instantaneous beam recovery times without the requirements for repeated beam scanning, as opposed to traditional codebook methods. Note that here identical data is transmitted on multiple component carriers in the same azimuth and elevation directions between a single MS and BS in line of sight (LoS) outdoor environments.

This paper is organized as follows. Section II presents the system model composed of the beamforming, signal, channel and blockage design models. Then the proposed link recovery scheme is introduced in Section III, followed by performance evaluation in Section IV, and finally conclusions in Section V.

Notations: $(.)^{H}$, $(.)^{T}$, and $\mathbb{E}(.)$ denote the Hermitian, the transpose, and the expected value, respectively.

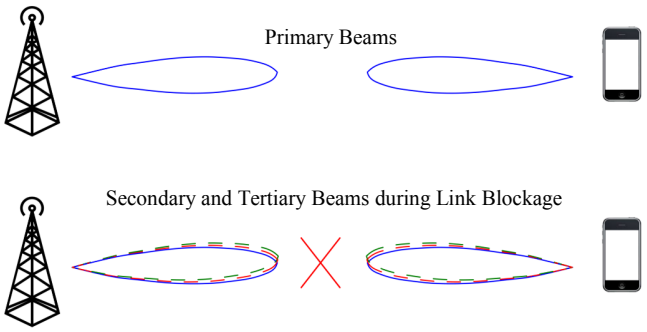

Fig.1. Proposed Beam Aggregation Link Recovery Scheme

II. System Model

A. Hybrid Beamformer

In general, circular antenna arrays provide several benefits compared to traditional uniform linear arrays (ULA) designs. Foremost, improved gains and directive half power beamwidths (HPBW) of less sidelobe lobe levels (SLL), as well as wider bandwidths and reduced mutual coupling. In addition, uniform circular arrays (UCA) provide [0, 2π] spatial scanning capabilities versus [0,π] scanning in ULA. Thus less number of antennas are required for the same directivity and gain levels, i.e., reduced power consumption and higher energy efficiencies. Furthermore, UCA features enhanced directivity and steady state gain over all directions, in particular at the endfire directions, whereas ULA suffers from degraded gains due to the beam broadening effect. Overall, UCA presents an appealing solution for beamforming architectures versus linear geometry approaches. Hence, the work here exploits UCA composed of microstrip rectangular patch antennas for hybrid beamforming (HBF) solutions.

In light of the above, consider a BS and MS equipped with a UCA geometry composed of N_{BS} and N_{MS} antennas, respectively, that are equally spaced on the *x*-*y* plane along a circular ring of radius *a*. Here $n_{BS} \in N_{BS}$ and $n_{MS} \in N_{MS}$ adjacent antennas are combined into $s=1,2,\ldots,S$ sections. Furthermore, each section *s* is connected to a single RF chain, *r*, to generate a single data stream.

Furthermore, the total number of RF chains at the MS is denoted by R_{MS}, i.e., $S=R_{MS}$, $R_{BS} << N_{BS}$, $R_{MS} << N_{MS}$. The composition of the proposed array and chains here form a hybrid beamformer (HBF) structure, which is constructed with limited number of data streams radiated by $b=1,2,\ldots,B$ simultaneous beams (beamforming and combining vectors) as depicted in Figure 2. Namely, the design of the pointing directions of *S* is determined by the precoding matrix at the BS, P_{BS}, i.e., composed of *p* precoding vectors. In particular, P_{BS} is constructed as $P_{BS} = P_{bb}P_{an}$, where P_{bb} and P_{an} are the baseband and analog precoding stages, i.e., $P_{bb}=S \times R_{BS}$ and $P_{an}=R_{BS} \times N_{BS}$ [7]. Figure 2 presents novel codebook structure based upon UCA that can be utilized in initial beam access and beam maintenance procedures, where wide beams are utilized in the initial stage. Note the fixed beamwidths at all spatial directions, which return in steady gain levels at all beamforming and combining vectors, as mentioned earlier.

Although the constructed HBF architecture here supports spatial multiplexing (MIMO), the RF chains are still used to support transmit diversity (redundant data streams), i.e., a form of diversity modulation. Consequently, signal aggregation and link recovery is achieved to compensate for signal degradation caused by blockage.

B. Signal Model

Assume a full-duplex downlink (DL) with channel state information (CSI) knowledge at the BS and MS. Hence the received signal model at the antenna lenses in the RF domain at the MS, i.e., analog side of the precoder, is given by:

$$\mathcal{Y}_{an} = P_{BS}\mathbf{H}z + w, \tag{1}$$

where **H** and *z* denote the complex channel and the primary reference control signal (PRCS), respectively. Also, *w* in Eq. (1) represents the additive white Gaussian noise (AWGN) component, $w \sim N(\partial, \sigma_w^2)$, with mean ∂ and variance σ_w^2. Meanwhile the overall received signal at the MS after the combiner stage, C_{MS}, at the baseband unit is formulated as [7]:

$$\mathcal{Y}_{bb} = P_{tr}C_{MS}^{H}P_{BS}\mathbf{H}z + C_{MS}^{H}w, \tag{2}$$

where P_{tr} is the transmitted signal power, and C_{MS} is the MS combiner. Furthermore, C_{MS} is composed of both baseband and analog combiners, i.e., $C_{MS} = C_{bb}C_{an}$. Meanwhile, the instantaneous received signal, $\mathcal{Y}_{c,p}^{inst}$, at the MS generated by the *p* and *c* beamforming and combining vectors, respectively, i.e., $p \in P_{BS}$, $c \in C_{MS}$, is expressed as:

$$\mathcal{Y}_{c,p}^{inst} = P_{tr}c^{H}p\mathbf{H}z + c^{H}w, \tag{3}$$

Now geometric channel model is adopted here due to the poor scattering propagation at mmWave bands [7],[8]:

$$\mathbf{H} = \sqrt{\frac{N_{BS}N_{MS}}{\Gamma_{bl}}}\sum_{k=1}^{K}\sum_{l=1}^{L}h_l V_{BS}U_{MS}^{H}, \tag{4}$$

where Γ_{bl} symbolizes the blockage path loss (dB,), h_l is the complex gain of the *l*-th path, for *L i.i.d.* total number of paths observed in *K* clusters, $L \in K$. Since this work assumes a scattering LoS environment, path gains are also assumed to be Rician-distributed, i.e., $h_l \sim \mathrm{R}(0, \zeta)$, where ζ is the ratio between power in the dominant first path component and the available power in other paths. Furthermore, V_{BS}, U_{MS}, in Eq. (4) denote in order, the array response vectors at the BS and MS, i.e., RF precoder of the HBF at which the channel is captured. Hence the overall response vector for the HBF

design at the MS is given by the RF precoding matrix and is expressed by the periodic array factor for the UCA at θ_s^{MS} azimuth and ϕ_s^{MS} elevation pointing directions (directions of main lobe peak, i.e., observation angles) for each section as per (likewise at the BS) [9],[10]:

$$U_{\mathrm{MS}}(\theta_s^{\mathrm{MS}},\phi_s^{\mathrm{MS}}) = \sum_{n=1}^{n_{\mathrm{MS}}} I_n \exp(jva(\cos\beta - \cos\beta_n^{\mathrm{MS}}) = \sum_{n=1}^{n_{\mathrm{MS}}} I_n \exp(jva(\cos(\phi_s^{\mathrm{MS}} - \mu), \quad (5)$$

$$\mu = \tan^{-1}\left(\frac{\sin\theta\sin\phi - \sin\theta_n^{\mathrm{MS}}\sin\phi_n^{\mathrm{MS}}}{\sin\theta\cos\phi - \sin\theta_n^{\mathrm{MS}}\cos\phi_n^{\mathrm{MS}}}\right). \quad (6)$$

The variables I_n and v from Eq. (5) in order are the amplitude excitation coefficient of the n-th antenna element, and the wave number, i.e., $v=2\pi/\lambda$, where λ is the wavelength, $\lambda=\alpha/f_\alpha$, where α is the speed of light and f_α is the operating frequency. Also, β_n^{MS} is the relative (progressive) phase shift for the n-th element at the MS.

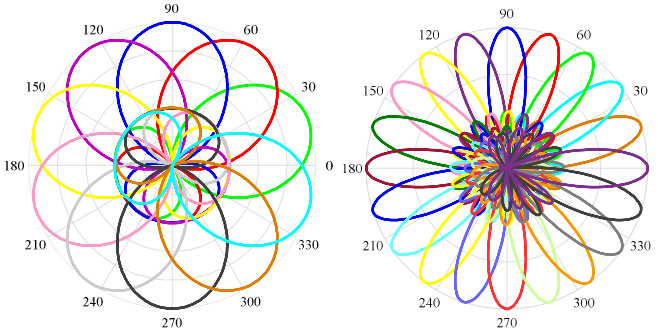

(a) Codebook Stage I (b) Codebook Stage II

Fig.2. Circular Array Cascaded Codebook

C. Blockage Model

As presented earlier, mmWave links are generally vulnerable to obstacles in the propagation paths which can result in link failure. Hence a blockage model that combines the transition from LoS-to-NLoS environments due to mobile obstacles is required. This path loss model leverages the blockage and distance parameters in [7],[11] as follows:

$$\Gamma_{bl} = \mathbb{I}[\mathbb{p}(d)]\Gamma_{\mathrm{LoS}}(d) + \mathbb{I}[1-\mathbb{p}(d)]\Gamma_{\mathrm{NLoS}}(d), \quad (7)$$

where $\mathbb{I}$ is an indicator function that determines the adopted path loss based upon the link-blockage state, i.e., $\mathbb{I}(x)=1$ *iff* $x=1$, and 0 otherwise. Furthermore, $\Gamma_{\mathrm{LoS}}(d)$ and $\Gamma_{\mathrm{NLoS}}(d)$ in Eq. (7) are the LoS and NLoS path losses, respectively, given by [12]:

$$\Gamma_{\mathrm{LoS}}(d) = 10\log_{10}(d_{ref}) + 10\delta_{\mathrm{LoS}}\log_{10}(d), \ \textit{for LoS}, \quad (8)$$

$$\Gamma_{\mathrm{NLoS}}(d) = 10\log_{10}(d_{ref}) + 10\delta_{\mathrm{NLoS}}\log_{10}(d), \ \textit{for NLoS}, \quad (9)$$

where d, d_{ref}, δ_{LoS} and δ_{NLoS} represent in order, the distance between the BS and MS, close-in reference distance (in meters), and path loss exponents (PLE) for the LoS and NLoS links.

Hence if a LoS link is not affected by the blockage, then the NLoS term decays to zero. Meanwhile, $\mathbb{p}(d)$ and $(1-\mathbb{p}(d))$ in Eq. (7) indicate the LoS and NLoS probabilities at distance d, i.e., $\mathbb{p}(d)=exp(-\varphi d)$, where φ is the blockage parameter representing the obstacles sizes and density. Note that the LoS link length is gauged by $1/\varphi$. Overall, this formulation indicates that the probability of denser obstacles increases with larger d values, and hence $\mathbb{p}(d)$ decreases.

III. Link Recovery Scheme

A. Initial Access Procedure

Consider a stationary BS and MS operating in LoS environment. Now both sides utilize the cascaded codebook structures with B predefined beams for initial random asynchronous beam search during the control-plane. This codebook defines B wide beams in the initial stage, where exhaustive beam scanning is conducted in each stage to determine the optimum beamforming and combining vectors. Note that the codebook beams in Figure 2 are generated by the circular array structure of Section II. Next, the optimum wide beam is selected for further refinement in latter stages for pencil beam transmission. Overall, a single narrow beam is selected for data-plane, whereas the other beams generated from R_{MS}-1 chains are deactivated to reduce power consumption levels. Overall, the best direction (primary beam) at the BS and MS returns the optimum beamforming and combining vectors at which the highest signal level, $\gamma_{c,p}^{pri}$ is observed at $(\theta_{pri},\phi_{pri})$ directions, i.e., exceeds certain channel capacity, γ_{th}, i.e.:

$$\gamma_{th} \geq max\ \log_2\left[\frac{P_{\mathrm{tr}}G_{\mathrm{MS}}G_{\mathrm{BS}}|h_l|^2}{\Psi T_0 \mathfrak{b}}\right], \quad (10)$$

where Ψ is the Boltzmann constant, T_0 is the operating temperature (in Kelvins), and $\mathfrak{b}$ is the contiguous channel bandwidth (in MHz). Also, G_{MS}, G_{BS} in Eq. (10) represent the gains at the MS and BS nodes, respectively, where $G_{\mathrm{MS}}=g_n\boldsymbol{U}_{\mathrm{MS}}$, $G_{\mathrm{BS}}=g_n\boldsymbol{V}_{\mathrm{BS}}$, and g_n is the gain for a single antenna element (e.g., microstrip rectangular patch). In general, this primary beam (link) corresponds to the direct LoS path used in the data-plane transmission, i.e.:

$$(c,p)_{opt} = max\ (\gamma_{c,p}^{pri}). \quad (11)$$

Once the primary beam establishment procedure is completed using $(c,p)_{pri}$, the subsequent data-plane stage is initiated. As mentioned earlier, the RF chains that radiates B other beams associated with other directions are deactivated to reduce power consumption. Hence the beamforming at this stage acts as single beam analog beamformer.

B. Instantaneous Link Recovery Scheme

Now if the highest signal level associated to the primary beams degrades during the data-plane (subsequent to the initial access association), i.e., below aforementioned instantaneous channel capacity threshold, then the residual RF chains R_{MS}-1 are activated. Hence their affiliated beams are radiated in the same direction of the primary beam to duplicate and enhance the signal at the failed primary beam. Namely, these beams yields in a secondary $\gamma_{c,p}^{sec}$ and tertiary $\gamma_{c,p}^{ter}$ aggregated (constructively added) signals at the receiver, i.e., overlaid

beams for signal duplication. Here the secondary and tertiary beam directions correspond to the primary beam direction, i.e.,

$$\theta_{pri} = \theta_{sec} = \theta_{ter} \text{ and } \phi_{pri} = \phi_{sec} = \phi_{ter} \quad (12)$$

Overall, the HBF in this paper radiates B number of instantaneous beams generated by R_{MS} RF chains. Hence once the primary link is degraded, the beams generated by these chains are utilized to generate redundant data streams, in contrast to spatial multiplexing. Note that $\gamma_{c,p}^{pri} > \gamma_{c,p}^{sec} > \gamma_{c,p}^{ter} > \gamma_{th} > \gamma_{rx}$, where γ_{th} and γ_{rx} in order, represent the threshold level exceeding channel capacity and receiver sensitivity.

Now at the receiving side, diversity combining schemes are used to constructively add the redundant signals from the aggregated beams. Since the secondary and tertiary paths correlated and received simultaneously, i.e., the spatial separation between the antenna elements is less than coherence distance, i.e., channel amplitude is similar for the secondary and tertiary paths, which results in dependent channels for the overlaid beams. Hence equal gain combining (EGC) scheme [7],[9] is applied here to combine signals from the secondary and tertiary beams, i.e., co-phased signals to provide combining diversity. Namely, EGC is applied to enhance the received signal from the secondary and tertiary beamforming (combining) vectors, expressed by:

$$\begin{aligned} \gamma_{c,p}^{EGC} &= \gamma_{c,p}^{EGC} + \gamma_{c,p}^{EGC} \\ &= P_{\text{tr}} c_{\text{sec}}^{\text{H}} p_{\text{sec}} h_l z + c_{sec}^{\text{H}} w + P_{\text{tr}} c_{\text{ter}}^{\text{H}} P_{\text{ter}} h_l z + c_{\text{ter}}^{\text{H}} w, \end{aligned} \quad (13)$$

where c_{sec}, p_{sec}, c_{ter} and p_{ter} denote the combining and beamforming vectors at the secondary and tertiary stages, respectively. Overall, this technique compensates for the received signal level and eliminates the requirements for iterative repeated beam scanning. As a result, the MS is not mandated to resume the control-plane and the communication session is maintained during link blockage. Namely, the signal level at the secondary beam vectors is denoted as $\gamma_{c,p}^{sec}$ and is associated with another pair of beamforming and combining vectors, i.e., $(c,p)_{sec}$. Additionally, the tertiary optimum signal $\gamma_{c,p}^{ter}$ is also determined as $(c,p)_{ter}$. Overall, these optimal links are exploited as redundant supplementary beams to enhance the received signal level once the link is degraded due to increased blockage.

IV. Performance Evaluation

The BS and MS operate in standalone mmWave network at f_a carrier frequency and BW channel bandwidth in outdoor environment. Table I illustrates the overall system parameter settings. Now the key metrics that evaluate the proposed recovery scheme are presented, in particular the received signal level and recovery times.

A. Received Signal Level

One key metric here is the received signal level, gauged by the SNR at various blockage parameter levels, φ, i.e., corresponding to obstacles of various densities (0.001-0.1), as per Figure 3. Initially, when the blockage parameter $\varphi = 0$, then the NLoS probability is $(1 - \mathbb{p}(d)) = 0$. Thus the MS and BS simply operate in LoS mode over a single primary beam. However, when $\varphi > 0$, the density and size of obstacles along the primary beam (link) increases, which results in severe signal degradation and link failure (NLoS operation).

Now at φ=0.001, the BS and MS operate in LoS settings and high SNR level is recorded, i.e., 6 dB. However, once the blockage density increases, the SNR starts to degrade significantly in transition to NLoS environment, e.g., at φ= 0.05 the SNR features 50% reduction at 3 dB, whereas the proposed scheme initiates beam aggregation to compensate for the SNR reduction, i.e., 5 dB.

TABLE I: SYSTEM PARAMETERS

Category	Parameters	Value
System	f_a(GHz), б (MHz), γ_{rx}(dBm)	38, 500, -110
Channel	∂, σ_w^2, ζ, d_{ref}, d	0, 1, 3, 5, 200
HBF	P_{tr}, g_n, N_{BS}, N_{MS}, a, R_{BS}, R_{MS}, $R_{\text{BS}}^{\text{act}}$, $R_{\text{MS}}^{\text{act}}$	30, 5, 16, 16,1 ,3, 3, 1, 1
PSS time	τ_{pss} (μs)	200
Path loss	δ_{LoS}, δ_{NLoS}	2, 4

Overall, the significant enhancement observed here maintains communication sessions at both control- and data- planes in the presence of blockage effects at near-instantaneous recovery times.

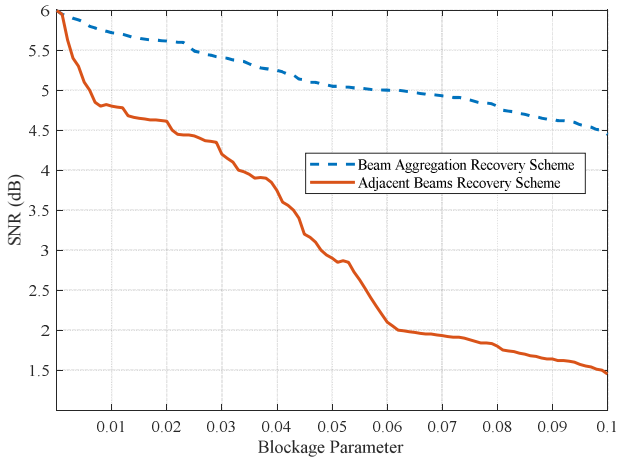

Fig.3. Signal-to-Noise Ratio at Various Blockage Levels

B. Link Recovery Times

Link recovery (re-access) times present crucial design aspect for mmWave beamforming-based transceivers. Now this value is defined as the time scan cycle required to determine alternative beamforming and combing vectors at the MS and BS, once the signal associated with the optimum beamforming and combining vectors is degraded due to blockage sensitivity (obstacles and increased path loss levels). Namely, it is defined as $T = Q\tau_{\text{PSS}}/R_{\text{MS}}^{\text{act}}$ (in microseconds), where Q is the total number of signal measurements at different beamforming and combining vectors (c,p) for detecting a new optimum direction, Also, the variables τ_{PSS} and $R_{\text{MS}}^{\text{act}}$, symbolize are the PSS duration and number of active RF chains at the MS, respectively. Figure 4 shows the link recovery times at various number of beamforming vectors that covers the entire spatial domain, i.e., $[0, 2\pi]$. For example, the proposed beam

aggregation scheme requires 200 ms to establish the redundant beams after increased blockage levels, hence maintaining the communication session with sufficient signal level. Here beam scanning is not required as the secondary and tertiary directions have already been determined based upon the direction of the primary beam. This merit eliminates the need for beam scanning during the recovery stage and introduces near-instantaneous recovery time.

Note that this value is similar for all number of beamforming vectors since no beam scanning is required, i.e., similar observation to the recovery times in [7]. Namely, once the signal affiliated with primary beam, the redundant aggregated beams are activated instantly in the direction of the optimum beam. Meanwhile, traditional schemes mandate scanning various directions to determine an alternative beam vectors. Such as the adjacent beam scanning recovery scheme that examines the neighboring directions of the degraded primary beam, i.e., 400 ms. Overall, the proposed scheme features near-instantaneous recovery times that are equal to the PSS duration, which presents 50% improvements to the adjacent beam recovery scheme in [6] and cascaded codebook structures [2]-[5] that in returns can result in connections drop since the scanning time exceeds the channel coherence time, hence control-plane can be restarted in this case.

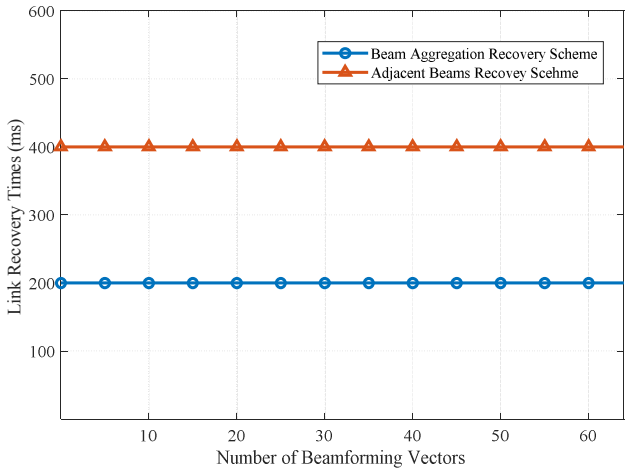

Fig.4. Link Recovery Times at various Beamforming Vectors

V. CONCLUSIONS

This paper proposes novel beam aggregation scheme for standalone mmWave cellular systems as part of the NR in 5G systems. First, a novel hybrid beamforming solution is presented based upon circular symmetric geometry array, where this beamformer is exploited for redundant data transmission at which equal gain combining is applied to aggregate the simultaneously received signals from the secondary and tertiary paths. Simulation results indicate that the proposed scheme exhibits near-instantaneous recovery times compared to traditional solutions at significantly enhanced received signal levels. Future efforts would investigate recovery schemes during MS high mobility and multi-user environments in standalone and non-standalone new radio networks.

REFERENCES

[1] International Mobile Telecommunications, "Minimum Requirements Related to Technical Performance for IMT-2020 Radio Interface", ITU-R Study Group 5, No. R15-SG05-C-0040, Feb. 2017, pp 6-7.

[2] M. Jasim, A. Aldalbahi, A. Khreishah, N. Ghani, "Hooke Jeeves search method for initial beam access in 5G mmWave cellular networks," *2017 IEEE 28th Annual International Symposium on Personal, Indoor, and Mobile Radio Communications (PIMRC)*, Montreal, QC, Canada, Oct. 2017.

[3] M. Jasim, N. Ghani, "Generalized pattern search for beam discovery in millimeter wave systems," *2017 IEEE 86th Vehicular Technology Conference (VTC-Fall)*, Toronto, ON, Canada, Sept. 2017.

[4] M. Jasim, N. Ghani, "Adaptive initial beam search for sparse millimeter wave channels," *2017 Wireless and Optical Communication Conference (WOCC)*, Newark, NJ, USA, April 2017.

[5] M. Jasim, N. Ghani, "Fast beam discovery for mmWave cellular networks," in *2017 IEEE Wireless and Microwave Technology Conference (WAMICON),* Cocoa Beach, FL, USA, April 2017.

[6] B. Gao *et al.*, "Double-link beam tracking against human blockage and device mobility for 60-GHz WLAN," *2014 IEEE Wireless Communications and Networking Conference (WCNC)*, Istanbul, Turkey, 2014.

[7] M. Jasim, M. Ababneh, N. Siasi, N. Ghani, "Hybrid beamforming for link recovery in millimeter wave communications," in *2018 IEEE Wireless and Microwave Technology Conference (WAMICON),* Clearwater, FL, USA, April 2018.

[8] A. Alkhateeb, O. El Ayach, G. Leus, R. W. Heath, "Channel estimation and hybrid precoding for millimeter wave cellular systems," *IEEE Journal of Selected Topics in Signal Processing*, Vol. 8, No. 5, Oct. 2014, pp. 831-846.

[9] W. Stutzman, G. Thiele, "Array Antennas," *Antenna Theory and Design*, 3rd Edition, John Wiley & Sons, 2012, pp. 294-295.

[10] C. Balanis, "Arrays: Linear, Planar and Circular," *Antenna Theory: Analysis and Design*, 3rd Edition, J. Wiley & Sons, 2005, pp. 290-304.

[11] T. Bai, V. Desai, R. W Heath, "Millimeter wave cellular channel models for system evaluation", *2014 International Conference on Computing, Networking and Communications (ICNC)*, Honolulu, HI, USA, Feb 2014.

[12] S. Sun *et al.*, "Propagation path loss models for 5G urban micro- and macro-cellular scenarios," *2016 IEEE 83rd Vehicular Technology Conference (VTC2016-Spring)*, Nanjing, China, May 2016.

[13] N. Siasi, N. I. Sulieman, R. D. Gitlin, "Ultra-Reliable NFV-based 5G Networks using Diversity and network coding," in *2018 IEEE Wireless and Microwave Technology Conference (WAMICON),* Clearwater, FL, USA, April 2018.